

Interfacial, Dynamic Mechanical, and Thermal Fiber Reinforced Behavior of MAPE Treated Sisal Fiber Reinforced HDPE Composites

Smita Mohanty,¹ Sanjay K. Nayak²

¹Central Institute of Plastics Engineering and Technology, Guindy, Chennai 600032, India

²Central Institute of Plastics Engineering and Technology, Bhubaneswar 751024, India

Received 28 December 2005; accepted 22 March 2006

DOI 10.1002/app.24799

Published online in Wiley InterScience (www.interscience.wiley.com).

ABSTRACT: The present article summarizes an experimental study on the mechanical and dynamic mechanical behavior of sisal fiber reinforced HDPE composites. Variations in mechanical strength, storage modulus (E'), loss modulus (E''), and damping parameter ($\tan \delta$) with the addition of fibers and coupling agents were investigated. It was observed that the tensile, flexural, and impact strengths increased with the increase in fiber loading up to 30%, above which there was a significant deterioration in the mechanical strength. Further, the composites treated with MAPE showed improved properties in comparison with the untreated composites. Dynamic mechanical analysis data also showed an

increase in the storage modulus of the treated composites. The $\tan \delta$ spectra presented a strong influence of fiber content and coupling agent on the α and γ relaxation process of HDPE. The thermal behavior of the composites was evaluated from TGA/DTG thermograms. The fiber-matrix morphology in the treated composites was confirmed by SEM analysis of the tensile fractured specimens. FTIR spectra of the treated and untreated composites were also studied, to ascertain the existence of type of interfacial bonds. © 2006 Wiley Periodicals, Inc. *J Appl Polym Sci* 102: 3306–3315, 2006

Key words: fibers; mechanical properties; DMA; SEM; TGA

INTRODUCTION

Fiber reinforced thermoplastic composites showed supremacy over conventional materials owing to ease of processing, fast production cycle and low tooling cost, thus making them most suitable material for automobile and electrical industries.¹ These composites are designed to perform in different static and dynamic conditions.² The enhanced material performance depends entirely on interfacial bond strength between the fibers and matrix.³ The matrix layer in contact with the fiber surface has different properties from the bulk matrix because of fiber/polymer interactions due to mechanical matrix immobilization of the chains, electrostatic forces, or chemical bonds in presence of internal stresses, voids, or micro cracks in the interlayer.⁴

Dynamic mechanical and thermal analysis have become widely used techniques for determining the interfacial characteristics of heterogeneous polymeric systems.⁵ DMA measurements conducted over a wide range of temperature helps to study the viscoelastic behavior of molten polymer systems and in particular the glass-transition region in the fiber reinforced composites. The temperature-dependent dynamic parameters such as dynamic modulus E^* , storage modulus E' ,

loss modulus E'' , and mechanical damping $\tan \delta$ provide an insight into the level of interactions between the polymer matrix and fiber reinforcement. Several studies have been carried out on the DMT properties of synthetic fiber reinforced and particulate filled composites to investigate the effect of addition of fillers, impact modifiers, coupling agents, compatibilizers, etc. on fiber matrix interface.^{6–17} However, extensive studies related to natural fibers as reinforcing agents have not been reported.^{18–21}

Ray et al.⁵ studied the dynamic mechanical and thermal characteristics of vinyl ester resin matrix reinforced with untreated and alkali-treated jute fibers. They observed a shift in T_g of the virgin matrix with the incorporation of alkali-treated jute fibers. Similar phenomenon has also been investigated by Rana et al.²² and Ghosh et al.²³ for compatibilized jute PP and epoxy systems. Existence of a secondary transition at a temperature higher than T_g has also been reported in the literature.^{24,25} This high-temperature peak was envisaged to be associated with the micro Brownian motion of the immobilized polymer molecules in the vicinity of solid surface.

Detailed investigations by Pothan et al.²⁶ on two, three, and four layered hybrid composites of banana/glass fiber woven fabric reinforced in polyester matrix revealed three peaks corresponding to resin, glass, and banana fiber from the loss modulus curves. Storage modulus and thermal transition temperature of

Correspondence to: S. K. Nayak (drsknayak@yahoo.com).

cianoethylated jute reinforced polyester composites have also been studied by Saha et al.²⁷ A pronounced effect of cyanoethylation of the fibers on T_g and magnitude of $\tan \delta$ peaks of the matrix polymer has been interpreted. Similarly, several investigations on physico-mechanical, thermal, and morphological characteristics of sisal fiber reinforced polymer matrix composites have been reported by various workers.^{28–34}

In the present investigation, the suitability of MAPE modified sisal as reinforcement in HDPE matrix and the viscoelastic behavior of the composites have been studied. A systematic investigation on the effect of fiber loading, MAPE concentration, and fiber treatment time was undertaken to obtain optimum mechanical strength. The composites were also subjected to periodic stress employing dynamic mechanical test, to investigate the variation of storage modulus, loss modulus, and damping properties as a function of temperature. The thermal stability of the composites was studied employing TGA/DTG whereas the fiber matrix morphology was analyzed through SEM. FTIR spectra implied the interfacial bonds between fibers and matrix of the composites.

EXPERIMENTAL

Materials

High density polyethylene (160A80) with a density of 0.96 g/cc and melt flow index of 8 g/10 min, obtained from M/s Gas Authority of India (GAIL), India, was used as the base polymer matrix. Sisal fibers, having an average fiber diameter of 40 μm , obtained from Kheonjhar (Orissa), India, were used as reinforcing agent.

Maleic anhydride grafted PE (MAPE), obtained from M/s Eastman Chemicals, Germany, under the trade name Epolene C₁₆ having < 0.1 wt % maleic anhydride, with M_w 26,000 and acid number 5, was used as coupling agent.

Composite fabrication

The fibers were detergent washed, dried in vacuum oven at 70°C for 24 h prior to composite preparation. To ensure easy blending of the fibers with the HDPE matrix, the detergent washed fibers were cut to an approximate fiber length of 6 mm, using an electronic fiber cutting machine.

Sisal/HDPE composites were prepared by melt mixing in Haake Torque Rheocord-9000 using roller blades and a mixing chamber with volumetric capacity of 69 cm³. The sample preparation was carried out in two stages. In the first stage, the untreated fibers along with HDPE were premixed at different weight percent of fiber loading (10, 15, 30, 45%) and fed into a preheated chamber at 160°C. The mixing was carried out for

10 min with a rotor speed of 25 rpm. In the second stage, the MAPE treated fibers (at 30% fiber loading) of variable concentration of MAPE (0.3, 0.5, 1, and 2%) were mixed with HDPE at the same condition of 160°C and 25 rpm rotor speed.

Subsequently, these premixes (untreated and treated) were brought to room temperature and compression molded using Delta Malikson Pressman 100T (India), at 150°C to produce sheets of 3 ± 0.1 mm thickness.

Test specimens were prepared from these sheets as per ASTM-D 638, 790, 256, and 570 using contour cut-copy milling machine; 6490 (Ceast, Italy) with calibrated templates.

Mechanical properties

Tensile testing

Specimens of virgin HDPE, untreated and treated composites of dimensions 165 × 13 × 3 mm, were subjected to tensile test as per ASTM-D-638, using Universal Testing Machine, LR-100K (Lloyd instruments, U.K). A crosshead speed of 100 mm/min and a gauge length of 50 mm were used for carrying out the test.

Flexural testing

The composite specimens, both untreated and treated along with virgin HDPE of dimensions 80 × 12.7 × 3 mm, were taken for flexural test, under three point bending, using the same Universal Testing Machine (UTM), in accordance with ASTM-D 790, at a crosshead speed of 1.3 mm/min and a span length of 50 mm.

Impact testing

Izod impact strength of the specimens having dimensions 63.5 × 12.7 × 3 mm was determined as per ASTM-D-256 with a notch angle of 45° and a "V" notch depth of 2.54 mm employing Impactometer 6545 (Ceast, Italy).

Five replicate specimens were evaluated at 23°C and 55% RH for each of the above tests, and the mean values were reported. Corresponding standard deviations along with the measurement uncertainty values for the experimental data showing maximum standard deviation is also included.

Dynamic mechanical properties

Specimens of virgin HDPE, untreated and treated composites having dimensions 27.4 × 3.1 × 3 mm were subjected to dynamic mechanical test using Rheometrics RDA-III (U.K). The measurements were carried out in the bending mode of the equipment and corresponding viscoelastic properties were determined as a function of temperature. The temperature range used

TABLE I
Effect of Fiber Loading on Mechanical Strength

Fiber (wt %)	Tensile strength (MPa)	SD	Tensile modulus (MPa)	SD	Elongation (%)	SD	Flexural strength (MPa)	SD	Flexural modulus (MPa)	SD	Impact strength (J/m)	SD
0	20.8	0.62	109.4	0.59	8.6	0.86	24.1	0.78	682.4	0.93	32.6	0.85
10	26.2	0.97	289.4	1.03	7.5	0.98	29.4 ± 1.13	1.08	784.3 ± 1.13	1.06	41.3	1.01
15	28.7	0.89	346.4	0.91	7.3	1.09	31.2	0.93	845.1	1.08	49.0	0.99
30	33.8	0.79	584.1	1.02	6.6	1.02	36.3	0.89	1725.0	0.89	57.6	1.03
45	26.7 ± 97 ^a	0.99	451.0	0.97	5.9 ± 1.27	1.13	30.0	0.78	1189.2	0.83	48.9 ± 1.43	1.19

^a Measurement uncertainty values as per A2LA guidelines.³⁵

in the present investigation was varied from -150 to 100°C, with a heating rate of 3°C/min, under nitrogen flow. The samples were scanned at a fixed frequency of 10 Hz, with a static strain of 0.2% and dynamic strain of 0.1%.

Interfacial properties

Scanning electron microscopy (SEM)

The morphology of the composites was studied employing scanning electron microscope (JEOL-JSM 5800, Japan). The tensile fractured surfaces of the composite specimens were gold sputtered (50 nm thickness) and dried for half an hour in vacuum at 100°C prior to study.

Fourier transformation infrared spectroscopy (FTIR)

FTIR spectra of virgin HDPE, MAPE copolymer, untreated and treated sisal HDPE composites were recorded using Perkin-Elmer 1720X (U.K) spectrometer. Each spectrum was obtained by co-adding 64 consecutive scans with a resolution of 4 cm⁻¹ within the range of 500–4000 cm⁻¹. The samples were studied using two different methods.

The FTIR analysis of virgin HDPE and MAPE copolymer were studied using cast film method. A xylene solution of maleated copolymer (MAPE) and HDPE were prepared separately in a beaker and dropped with a pipette on a NaCl disk. A uniform and continuous film was formed on the disk until the solvent was completely evaporated.

Conversely, the FTIR spectra of the composite samples were studied employing KBr pellet technique. One milligram of finely ground composite sample was mixed with about 100 mg of dried KBr powder within a sample set and a pressure of 69–103 MPa was applied to yield a transparent disk.

Thermal properties

Sisal fiber, virgin HDPE, and the composites, both untreated and treated, were subjected to thermogravimetric analysis using Perkin-Elmer Pyris-1, USA equipment. Samples of ≤ 5 mg weight were scanned from 40 to 900°C at a heating rate of 20°C/min in nitrogen atmosphere and the corresponding weight loss was recorded.

RESULTS AND DISCUSSION

Mechanical properties

Effect of fiber loading

The variation of mechanical strength as a function of fiber loading is represented in Table I. It was observed that the mechanical properties of the untreated sisal-HDPE composites increased linearly with the increase in fiber loading from 10 to 30%. The composites prepared at 30% fiber loading exhibited higher tensile strength of 33.8 MPa, flexural strength of 36.3 MPa, and impact strength of 57.6 J/m as compared with virgin HDPE. Corresponding tensile and flexural modulus also increased to the tune of 433 and 153%. This

TABLE II
Effect of Concentration of MAPE on Mechanical Strength of the Composites at 30% Fiber Loading Treated for 7 Minutes

MAPP concentration (%)	Tensile strength (MPa)	SD	Tensile modulus (MPa)	SD	Elongation (%)	SD	Flexural strength (MPa)	SD	Flexural modulus (MPa)	SD	Impact strength (J/m)	SD
0.0	33.8	0.79	584.1 ± 1.30	1.02	6.6	1.02	36.3	0.89	1725.0	0.89	57.6	1.03
0.3	37.7	0.93	1079.7	0.87	5.5	1.0	46.9	1.01	2376.1 ± 1.38	1.12	59.7	0.85
0.5	39.9	0.95	1189.0	0.63	5.4 ± 1.21	1.12	49.3	0.96	2597.8	0.99	62.6	0.94
1.0	44.3	0.87	1243.8	0.92	5.2	0.99	59.2	0.98	2856.3	1.05	68.4 ± 1.42	1.04
2.0	36.8 ± 1.27	1.01	1122.0	0.91	4.8	1.23	38.6 ± 1.42	1.03	2201.0	0.97	60.3	0.97

TABLE III
Effect of Time Period Variation of MAPE on Mechanical Strength of the Composites at 30% Fiber Loading and 1% MAPE Concentration

Treatment time of MAPP (min)	Tensile strength (MPa)	SD	Tensile modulus (MPa)	SD	Elongation (%)	SD	Flexural strength (MPa)	SD	Flexural modulus (MPa)	SD	Impact strength (J/m)	SD
3	41.2	1.01	1101.2	0.95	4.5	0.87	47.1	1.01	2354.8	0.91	62.8	1.03
5	42.3 ± 1.20	1.10	1209.8	0.87	5.2	0.71	51.9	0.83	2687.6	1.01	64.3 ± 1.12	1.12
7	44.3	0.87	1243.8	0.92	5.2 ± 1.31	0.99	59.2	0.98	2856.3	1.05	68.4	1.04
10	36.8	0.99	1013.7 ± 1.32	1.08	4.4	0.95	49.1 ± 1.41	1.21	2245.0 ± 1.35	1.12	59.8	0.98

phenomenal increase in the mechanical strength is primarily attributed to reinforcing effect imparted by the fibers, which allowed a uniform stress distribution from continuous polymer matrix to dispersed fiber phase.³⁶ However, the mechanical properties declined with the increase in the fiber loading from 30 to 45%. A decrease of 27% in tensile, 21% in flexural, and 18% in impact strengths was noticed. A similar decrease in tensile and flexural modulus to the tune of 30 and 45% was also observed as compared with the virgin HDPE. Elongation of the virgin matrix also reduced with reinforcement. This decrease in the mechanical properties at high fiber loading implied poor fiber–matrix adhesion, which promoted microcrack formation at the interface as well as nonuniform stress transfer because of fiber agglomeration within the matrix.³⁷ Similar investigations have also been reported by Mohanty et al.³³ for jute polyester amide composites in which the broken fiber ends caused crack initiation and potential composite failure at 53% fiber loading. Rana et al.³² have also investigated a decrease in the impact strength by 177% in jute/PP composites as the fiber loading was increased from 30 to 60%. Similar facts are also substantiated in our experimental results.

Effect of MAPE treatment

The hydroxyl and the other polar groups located in the branched heteropolysaccharides, present in the sisal fibers, are the active sites of water absorption, which results in incompatibility with the hydrophobic HDPE matrix leading to poor composite properties. To reduce the surface hydrophilicity, sisal fibers were treated with MAPE. The maleic anhydride groups of MAPE covalently links with the hydroxyl groups of the fibers forming an ester linkage. Furthermore, the nonpolar part (PE) of MAPE becomes compatible with the virgin matrix, lowers the surface energies of the fibers, thereby increasing its wettability and dispersion within the matrix. As implied from the test results reported in Table II, all the treated composites (at 30% fiber loading) exhibited improved mechanical strength in comparison to the untreated composite at the same weight percent of fiber content. The composites prepared using 1% MAPE concentration showed considerable enhancement in tensile, flexural and impact

strengths with a value of 31, 63.2, and 19%, respectively, as compared with the 30% untreated composite. Similarly, the tensile and flexural modulus increased to the tune of 112 and 66%. This phenomenon is probably due to increase in interfacial adhesion between the fibers and the matrix with the addition of MAPE. Further, increase in the MAPE concentration from 1 to 2%, resulted in a marginal decrease in the mechanical properties. Gassan et al.³⁸ have also reported similar behavior for jute and flax fiber reinforced PP composites. This behavior may be attributed to the migration of excess MAPE around the fibers, causing self-entanglement among themselves rather than the polymer matrix resulting in slippage of the fibers within the matrix.³⁹

Effect of time period on impregnation

The variation of mechanical strength as a function of fiber treatment time is represented in Table III. An optimized sisal loading of 30% and MAPE concentration of 1% was maintained for the evaluation of the mechanical strength as a function of treatment time period.

As implied from the test results reported in Table III, an optimum mechanical performance was obtained with the composites treated for a period of 7 min. There was an increase of 8% in tensile, 26% in flexural, and 9% impact strength with the increase in treatment time period of MAPE from 3 to 7 min. Corresponding tensile and flexural modulus also increased to the tune of 13% and 21.2%, respectively. However, with a further increase in fiber treatment time from 7 to 10 min, deterioration in the mechanical properties was observed. Similar behavior was also observed in jute fiber reinforced HDPE composites with an increase in treatment time from 5 to 10 min.⁸ A decrease of 20.3% in tensile,

TABLE IV
Flexural and Storage Modulus of Virgin HDPE, Untreated and Treated Composites

Sample	Flexural modulus (MPa)	Storage modulus (MPa)
HDPE virgin	682.4	9.3 E + 08
Untreated	1742.0	1.3 E + 09
Treated	1243.8	1.6 E + 09

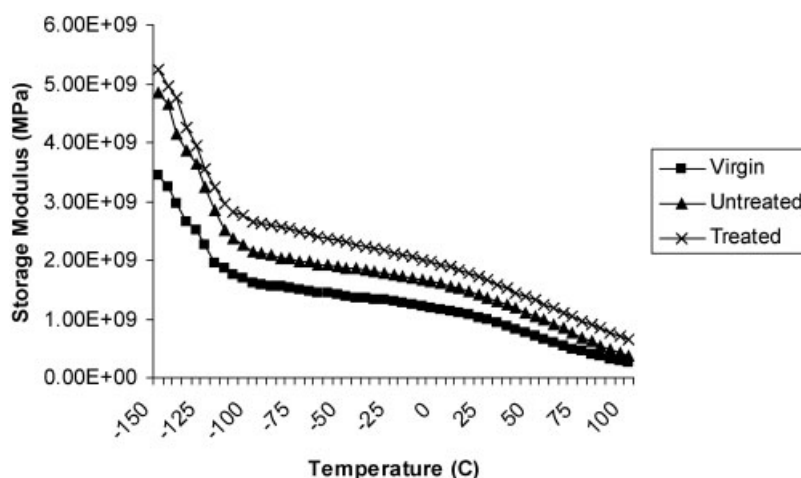


Figure 1 Variation of storage modulus with temperature.

21% in flexural, and 15.4% in impact strength was observed. A decrease in tensile (23%) and flexural modulus (27.2%) and elongation (20%) was also observed. This may be due to loss of strength of sisal fibers owing to their chain scission at high temperature on prolonged heating for a longer duration of 10 min. Similar behavior has been confirmed with the extensive investigations reported by Tripathy et al. on jute and sisal fiber reinforced PP composites.^{18,34}

The untreated composite (with 30% sisal loading) and treated composite (30% sisal loading with 1% MAPE concentration treated for a period of 7 min) were chosen for further characterization studies.

Dynamic mechanical properties

Storage modulus (E')

The storage modulus (E') is closely related to the load bearing capacity of a material and is analogous to the

flexural modulus (E) measured as per ASTM-D 790.²⁷ A comparative account of E' and E of virgin HDPE, untreated and treated composite evaluated at 30°C is represented in Table IV. The variation of storage modulus as a function of temperature is graphically enumerated in Figure 1. It is evident from Figure 1 that there was a notable increase in the modulus of virgin matrix with the incorporation of sisal fibers. This is probably due to increase in the stiffness of the matrix with the reinforcing effect imparted by the fibers that allowed a greater degree of stress transfer at the interface.³⁰ The flexural modulus E also increased by 76%, which revealed an increase in rigidity of the virgin matrix with the addition of the fibers. A similar increase in E and E' was also observed in the treated composites. The composite comprising 1% MAPE treated fibers and 30% loading showed nearly 191.2% increase in flexural modulus and 21% in storage modulus. This behavior is primarily attributed to improved interfa-

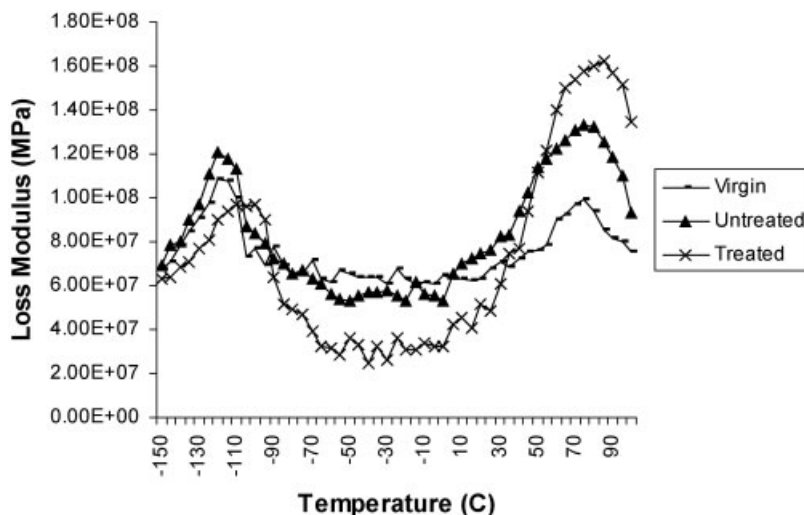


Figure 2 Variation of loss modulus with temperature.

TABLE V
Temperature Maximum of γ and α Peak and Loss Modulus of Virgin HDPE, Untreated and Treated HDPE Sisal Composites

Sample	γ ($^{\circ}\text{C}$)	E'' (MPa)	α ($^{\circ}\text{C}$)	E'' (MPa)
HDPE virgin	-120	1.08 E + 08	78	9.66 E + 07
Untreated	-100.5	1.11 E + 08	85	1.33 E + 08
Treated	-96.4	9.72 E + 07	91	1.62 E + 08

cial adhesion between the fibers and the matrix. In all the samples, the storage modulus decreased with the increase in temperature and there was a significant fall in the regions between -40 and 60°C . However, the rate of fall of the matrix modulus was compensated by the interactions caused in presence of fibers in the filled composites, which further shows an increase in thermal stability of the virgin matrix with the addition of fibers.

Loss modulus (E'')

HDPE shows two relaxation peaks at -110°C (γ) and 80°C (α), respectively.⁴⁰ The α relaxation is associated with the chain segment mobility in the crystalline phases, which is probably due to reorientation of defect areas in the crystals. The γ relaxation corresponds to the glass transition (T_g) of HDPE matrix and is related with the amorphous phase. The β transition of HDPE is not visible because of the absence of the branches. In the present investigation, the γ and α relaxation of virgin HDPE, untreated and treated composites have been studied from the loss modulus curves represented in Figure 2.

The γ and α relaxation peak of virgin matrix was detected around -109.8 and 80°C , respectively. In case of untreated composite, the primary transition peak i.e., T_g shifted to a marginally high temperature (-100.5°C).

This is primarily attributed to the segmental immobilization of the matrix chains at the fibers surface.⁴¹ The loss modulus corresponding to the T_g in the untreated composites also increased marginally to about 4% as compared with the virgin matrix. The composites comprising treated fibers with 1% MAPE showed an additional shift in T_g to a comparatively higher temperature (-96.4°C), which indicates enhanced interfacial adhesion between the fibers and the matrix, achieved due to coupling effect of MAPE. The loss modulus value at this temperature, however, decreased to the tune of 43%, thereby indicating the presence of a genuine interface.⁴⁰

The α relaxation peak of HDPE also exhibited a marginal shift to high temperature regions with the incorporation of fibers and MAPE. Corresponding loss modulus at this temperature increased accordingly, with the viscous dissipation²⁷ being maximum for the treated composite and minimum for the matrix polymer. The higher modulus at this temperature is probably due to the presence of sisal fibers that reduced the flexibility of the material by introducing constraints on the segmental mobility of polymeric molecules at the relaxation temperature.¹³ Further, broadening of the PE transition regions was observed in the untreated and treated composites, which is attributed to inhibition of the relaxation process within the composites with the addition of fibers.¹¹ In all the other regions, the untreated composite showed similar behavior as the virgin matrix. The temperature maximum of α and γ relaxation peak of virgin HDPE, untreated and treated composite and the corresponding loss modulus values at this temperature is represented in Table V.

Loss tangent ($\tan \delta$)

The ratio of loss modulus to storage modulus is measured as the mechanical loss factor or $\tan \delta$. The damp-

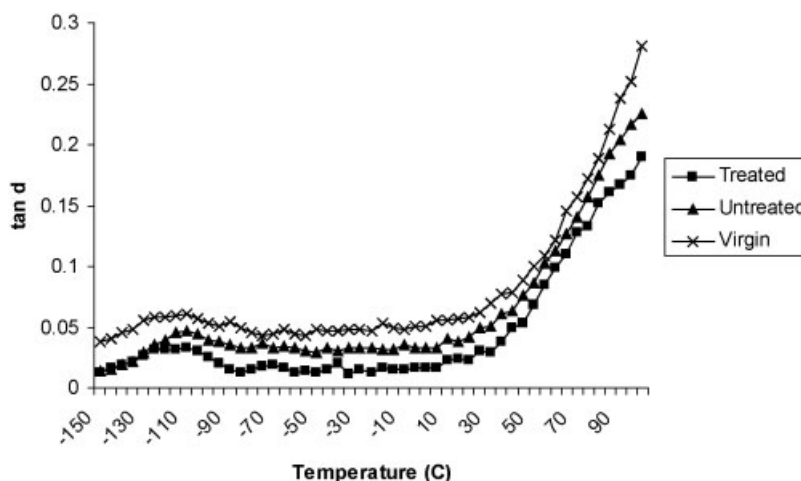


Figure 3 Variation of $\tan \delta$ with temperature.

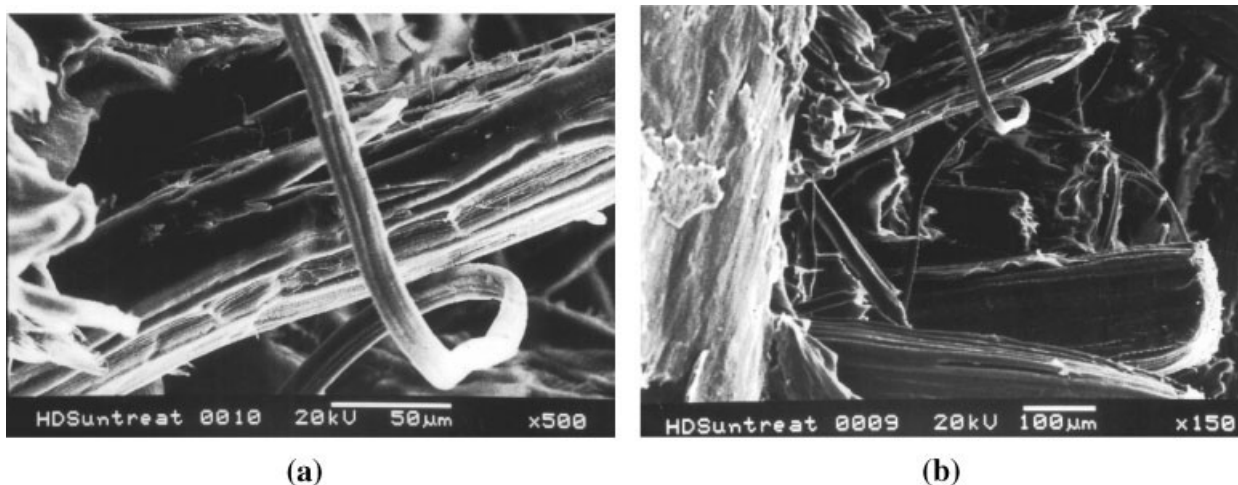


Figure 4 (a) SEM micrograph of untreated sample at a magnification of 50 μm . (b) SEM micrograph of untreated sample at a magnification of 100 μm .

ing properties of the material give the balance between the elastic phase and viscous phase in a polymeric structure. In the present investigation, the variation of $\tan \delta$ as a function of temperature is depicted in Figure 3. The damping peak in the treated composites showed a decreased magnitude of $\tan \delta$ in comparison with virgin HDPE and untreated composite. This is because the fibers carry a greater extent of stress and allow only a small part of it to strain the interface. Therefore, energy dissipation will occur in the polymer matrix and at the interface with a stronger interface characterized by less energy dissipation.⁴² Further in comparison to virgin HDPE, the $\tan \delta$ peak of untreated composites exhibited lower magnitude, which in turn showed a higher magnitude when compared with the treated composites. This envisages that a composite material with poor interfacial bonding between the fibers and matrix will tend to dissipate more energy, showing

high magnitude of damping peak in comparison to a material with strongly bonded interface,¹⁴ which is further substantiated by our experimental results.

Interfacial properties

Scanning electron microscopy

The morphology of the tensile fractured surfaces of untreated and treated composites are illustrated in Figures 4(a,b), 5(a,b), respectively. From Figure 4(a,b), it is evident that in the untreated composite, there are large number of gaps between the fibers and the matrix resulting from fiber pullouts. This indicates poor interfacial adhesion and inadequate wetting of the untreated fibers within the HDPE matrix, which is probably due to a large difference in the surface energies between the fibers, and the matrix. Conversely, MAPE treated composites manifested improved fiber

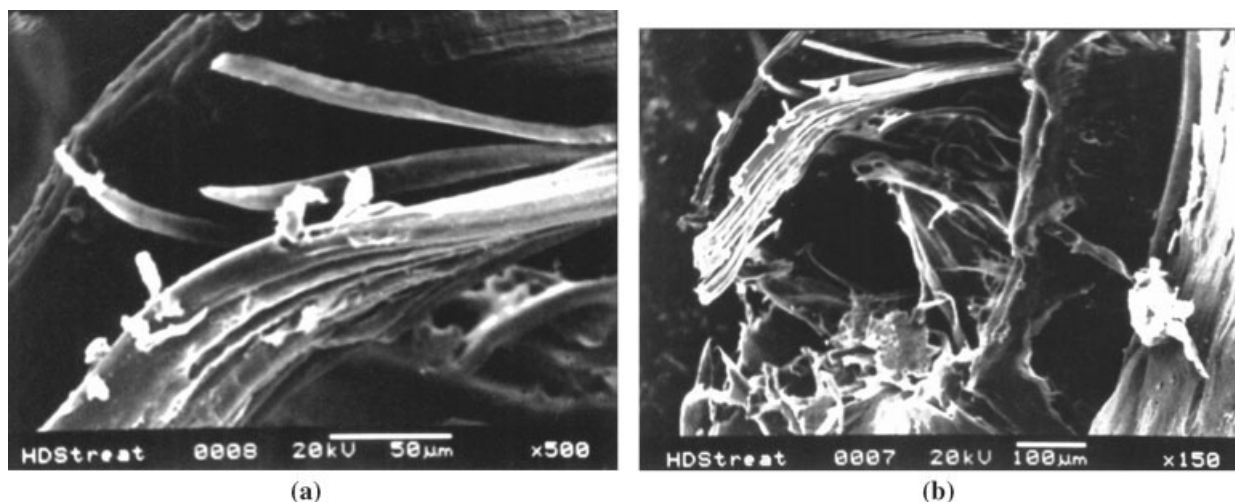


Figure 5 (a) SEM micrograph of MAPE treated sample at a magnification of 50 μm . (b) SEM micrograph of MAPE treated sample at a magnification of 100 μm .

matrix adhesion. As implied from Figures 5(a) and 5(b), the treated fibers are uniformly coated by layers of matrix material that considerably reduced the gaps between them. It was also observed that the layers of matrix material were pulled out together with the fibers during tensile fracture, which further substantiates cohesive coupling between the MAPE treated fibers and HDPE matrix.⁴⁰

Fourier transformation infrared spectroscopy

FTIR spectra of virgin HDPE and MAPE copolymer is depicted in Figure 6(a). It is evident that the backbone molecule polyethylene presents a strong peak of ($-C-H$) corresponding to 2923 and 1466 cm^{-1} with a moderate peak of ($-CH_2-$) around 720 cm^{-1} . Methyl groups ($C-CH_3$) also presented a significant peak at 2850 cm^{-1} . MAPE copolymer exhibited characteristic

peaks between 1800 and 1700 cm^{-1} [Fig. 6(b)], respectively. Bands corresponding to cyclic anhydrides were also observed within the range of 1800 and 1700 cm^{-1} , separated by about 60 cm^{-1} . The peak at low frequency of 1717 cm^{-1} was more intense than at high frequency of 1790 cm^{-1} . Figure 6(c) depicts the FTIR spectra of untreated and MAPE treated composites, respectively. As observed from the figure, the untreated composites exhibited a peak around 3400 cm^{-1} , which was mainly due to absorption of water by sisal fiber. Similar phenomenon was also observed in case of the MAPE treated composites. However, the treated composites displayed a strong band corresponding to 2931 and 2844 cm^{-1} , respectively, indicating the characteristic spectra of PE. Furthermore, a peak observed around 1751 cm^{-1} in these composites confirms the presence of ester linkage at the interface. The formation of ester linkage at the interface have also been reported by

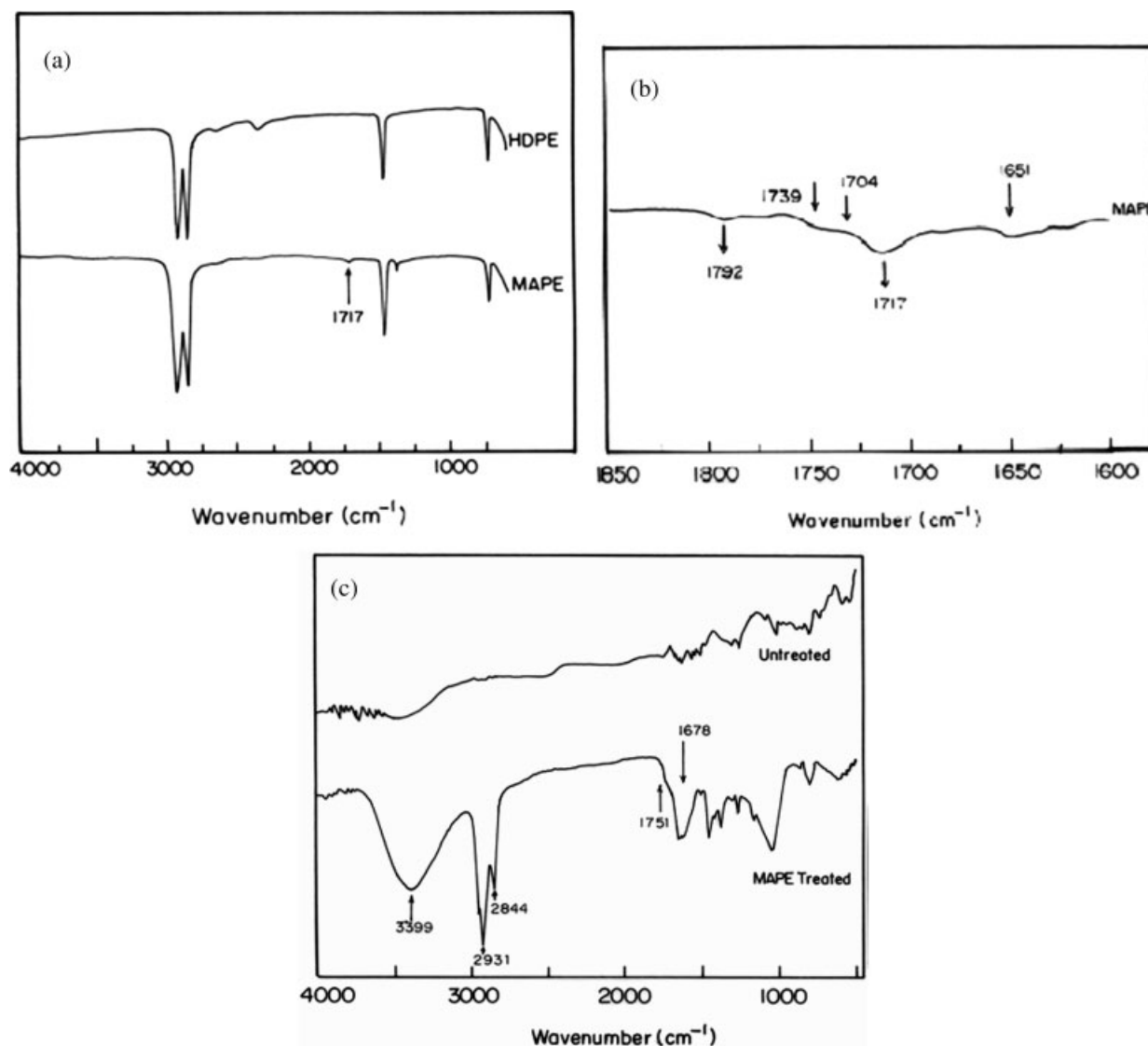


Figure 6 (a) FTIR spectra of virgin HDPE and MAPE copolymer, (b) FTIR spectra of MAPE copolymer, (c) FTIR spectra of untreated and MAPE treated composites.

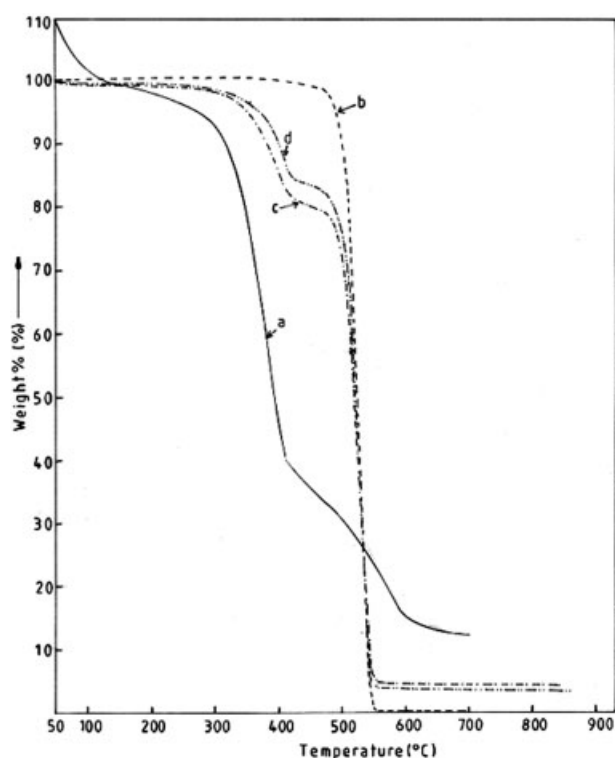


Figure 7 TGA of (a) sisal fiber, (b) virgin HDPE, (c) untreated composite, (d) treated composite.

Mohanty et al.¹⁸ and Botev et al.¹⁰ for jute and basalt fiber reinforced PP composites, respectively. The featured peak of cyclic anhydrides appeared at 1717 cm^{-1} , thus suggesting the existence of free or ungrafted maleic anhydride groups at the interface, which is probably due to limitation on graft polymerization (Lu et al.⁴³).

Thermal properties

The TGA and DTG curves of HDPE, sisal fiber, untreated and treated sisal/HDPE composites are depicted in Figures 7 and 8, respectively. It was observed that the thermal degradation of all the samples has taken place within the programmed temperature range of 30–900°C. In case of sisal fiber [Fig. 7(a)], dehydration and degradation of lignin occurred between 40 and 275°C and maximum percentage of cellulose decomposed at a temperature of 380°C [Fig. 8(a)]. The decomposition of virgin HDPE started at 430°C and nearly 100% decomposition occurred at 515°C [Fig. 8(b)]. This decomposition temperature range of HDPE was comparatively higher than that of the fibers. For the untreated sisal/HDPE composites prepared at 30% fiber loading [Fig. 7(c)], the initial peak between 320.1 and 394.3°C with a maximum at 367.5°C corresponds to a weight loss of about 20%. This was probably due to dehydration from cellulose unit and thermal cleavage of glycosidic linkage by

transglycosylation and scission of C—O and C—C bonds. The second decomposition occurred between 461 and 538°C with the main decomposition temperature as revealed from DTG curves around 522.5°C [Fig. 8(c)]. The weight loss at 522.5°C was about 76%, which is primarily attributed to aromatization, involving dehydration reactions. Similar results have also been reported by George et al. for PALF fiber reinforced LDPE composites.³⁹ At 515°C, HDPE [Fig. 8(b)] got completely decomposed while in the untreated composite a charred residue of carbonaceous products of 3.22% was left.³² The major decomposition of hemicellulose, α cellulose, and HDPE resin occurred between 482 and 587°C.

The treated composite [Fig. 7(d)] in contrast displayed a initial peak at 373.8°C because of dehydration from the cellulose unit and thermal cleavage and scission of C—O and C—C bonds. The loss in weight of the sample at this stage was 18%. The second decomposition temperature as revealed from the thermogram [Fig. 7(d)] was detected around 471.3°C with a weight loss of about 72.58%, and the main decomposition temperature was noticed around 530.9°C as revealed from the DTG thermogram [Fig. 8(d)]. The weight of the charred residue left at 530°C was about 4.81%. The major decomposition range was 479.7–598.7°C, which was almost same as in the untreated sisal/HDPE composite. However, the decomposition temperature in the first zone for the MAPE treated composites was

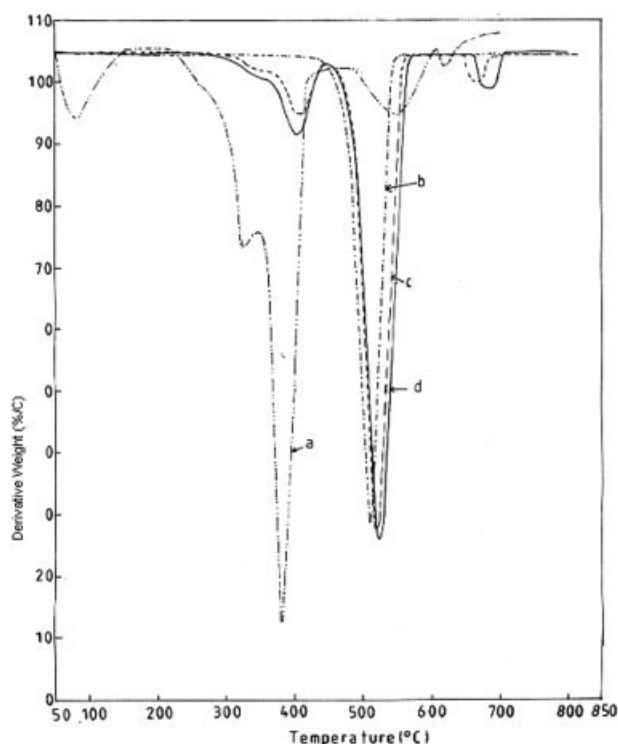


Figure 8 DTG of (a) sisal fiber, (b) virgin HDPE, (c) untreated composite, (d) treated composite.

higher than that of the untreated composites. The percentage of weight loss in case of MAPE treated composites in both the zones was also lower, which indicates a higher thermal stability of the composites comprising MAPE treated fibers.

CONCLUSIONS

The mechanical, dynamic mechanical and thermal properties of HDPE: sisal fiber composites have been investigated. The composites prepared with 30% sisal fiber treated in 1% MAPE showed optimum mechanical strength. The mechanical findings were corroborated with morphological evidence and DMA studies. Storage modulus vs. temperature plots also showed an increase in the magnitude of the peaks with fiber reinforcement and addition of MAPE. The damping properties of the treated and untreated composites, however, decreased in comparison with the virgin matrix. TGA and DTG thermograms displayed an increase in the thermal stability of HDPE matrix with fiber reinforcement and MAPE treatment. On the basis of these studies, it can be concluded that sisal fibers could effectively reinforce HDPE matrix when used in an optimal concentration of fibers and coupling agents.

References

1. Ma, C. C. M. First Asian Australasian Conference on Composite Materials (ACCM-I), Osaka, Japan, 1998; p 205.
2. Hashmi, S. A. R.; Kitano, T.; Chand, N. *Polym Compos* 2003, 24, 149.
3. Karger-Kocsis, J. *Polypropylene: Structure, Blends and Composites*, Vol. 3.; Chapman and Hall: London, 1995.
4. Calleja, R. D.; Ribelles, J. L. G.; Pradas, M. M.; Greus, A. R.; Colomer, F. R. *Polym Compos* 1991, 12, 428.
5. Ray, D.; Sarkar, B. K.; Das, S.; Rana, A. K. *Compos Sci Technol* 2002, 62, 911.
6. Vajrasthira, C.; Amornsakchai, T.; Limcharoen, B. *J Appl Polym Sci* 2003, 87, 1059.
7. Rout, J.; Tripathy, S. S.; Mishra, M.; Mohanty, A. K.; Nayak, S. K. *Polym Compos* 2002, 22, 468.
8. Mohanty, S.; Verma, S. K.; Tripathy, S. S.; Nayak, S. K. *Int J Plast Technol* 2003, 6, 75.
9. Bikiaris, D.; Matzinos, P.; Prinos, J.; Flaris, V.; Larena, A.; Panayiotou, C. *J Appl Polym Sci* 2001, 80, 2877.
10. Botev, M.; Betchev, H.; Bikiaris, D.; Panayiotou, C. *J Appl Polym Sci* 1999, 74, 523.
11. Woo, E. M.; Seferis, J. C. *Polym Compos* 1991, 12, 273.
12. Beaudoin, O.; Bergeret, A.; Quantin, J. C.; Crespy, A. *Polym Compos* 2002, 23, 87.
13. Lopez Manchado, M. A.; Biagiotti, J.; Kenny, J. M. *Polym Compos* 2002, 23, 779.
14. Ashida, M.; Noguchi, T. *J Appl Polym Sci* 1984, 29, 661.
15. Lewis, T. B.; Nielsen, L. E. *J Appl Polym Sci* 1970, 11, 1449.
16. Kubat, J.; Rigdahl, M.; Welander, M. *J Appl Polym Sci* 1990, 39, 1527.
17. Sohn, M. S.; Kim, K. S.; Hong, S. H.; Kim, J. K. *J Appl Polym Sci* 2003, 87, 1595.
18. Tripathy, S. S.; Mohanty, S.; Verma, S. K.; Nayak, S. K. *J Appl Polym Sci* 2004, 94, 1336.
19. Alfthan, E.; de Ruvo, A.; Brown, W. *J Reinforc Plast Compos* 1993, 12, 139.
20. Joseph, S.; Sreekala, M. S.; Thomas, S. *Int J Plast Technol* 2002, 5, 28.
21. Aurich, T.; Mennig, G. *Int J Plast Technol* 2002, 5, 9.
22. Rana, A. K.; Mitra, B. C.; Banerjee, A. N. *J Appl Polym Sci* 1999, 71, 531.
23. Ghosh, P.; Bose, N. R.; Mitra, B. C.; Das, S. *J Appl Polym Sci* 1997, 62, 2467.
24. Verghese, K. N. E.; Jensen, R. E.; Lesko, J. J.; Ward, T. C. *Polymer* 2001, 42, 1633.
25. Hon David, N. S.; Shiraishi, N. *Wood and Cellulose Chemistry*; Marcel Dekker: New York, 1991.
26. Pothan, L. A.; Potschke, P.; Thomas, S. In *Proceedings of the ACUN-3 (Technology Convergence in Composite Application)*, University of South Wales, Sydney, February 5-9, 2001; p 452.
27. Saha, A. K.; Das, S.; Bhatta, D.; Mitra, B. C. *J Appl Polym Sci* 1999, 71, 1505.
28. Karmaker, A. C.; Youngquist, J. A. *J Appl Polym Sci* 1996, 62, 1147.
29. Gassan, J.; Bledzki, A. K. *Polym Compos* 1999, 20, 604.
30. Dash, B. N.; Rana, A. K.; Mishra, H. K.; Nayak, S. K.; Mishra, S. C.; Tripathy, S. S. *Polym Compos* 1999, 20, 62.
31. Karmaker, A. C.; Schneider, J. P. *J Mater Sci Lett* 1996, 15, 201.
32. Rana, A. K.; Mandal, A.; Bandyopadhyay, B. *Compos Sci Technol* 2003, 63, 801.
33. Mohanty, A. K.; Khan, M. A.; Hinrichsen, G. *Compos A* 2000, 31, 143.
34. Tripathy, S. S.; Mohanty, S.; Verma, S. K.; Nayak, S. K. *J Reinforc Plast Compos* 2004, 23, 625.
35. Adams Thomas, M. *A2LA Guidelines for Estimation of Measurement Uncertainty in Testing*, 2002; p 1.
36. Colom, X.; Carrasco, F.; Pages, P.; Canavate, J. *Compos Sci Technol* 2003, 63, 161.
37. Thwe, M. M.; Liao, K. *J Mater Sci Lett* 2003, 38, 363.
38. Gassan, J.; Bledzki, A. K. *Compos A* 1997, 28, 1001.
39. Rana, A. K.; Mandal, A.; Mitra, B. C.; Jacobson, R.; Rowell, R.; Banerjee, A. N. *J Appl Polym Sci* 1998, 69, 329.
40. John, B.; Varughese, K. T.; Oommen, Z.; Potschke, P.; Thomas, S. *J Appl Polym Sci* 2003, 87, 2083.
41. George, J.; Bhagawan, S. S.; Thomas, S. *J Therm Anal* 1996, 47, 1121.
42. Felix, J. M.; Gatenholm, P. *J Appl Polym Sci* 1991, 42, 601.
43. Lu, J. Z.; Wu, Q.; Negulescu, I. I. *Wood Fiber Sci* 2002, 34, 434.